AIP | Journal of Applied Physics

# Strain effect caused by substrates on phase separation and transport properties in Pr0.7(Ca0.8Sr0.2)0.3MnO3 thin films

Y. Y. Zhao, F. X. Hu, J. Wang, L. Chen, W. W. Gao et al.

Citation: J. Appl. Phys. **111**, 07D721 (2012); doi: 10.1063/1.3678297
View online: http://dx.doi.org/10.1063/1.3678297
View Table of Contents: http://jap.aip.org/resource/1/JAPIAU/v111/i7
Published by the American Institute of Physics.

## Related Articles

High frequency clipper like behavior of tri-layer nickel oxide stack
Appl. Phys. Lett. 100, 152113 (2012)

Electrical and optical properties of sputtered amorphous vanadium oxide thin films
J. Appl. Phys. 111, 073522 (2012)

Resistive switching characteristics of solution-deposited Gd, Dy, and Ce-doped ZrO2 films
Appl. Phys. Lett. 100, 143504 (2012)

Local resistive switching of Nd doped BiFeO3 thin films
Appl. Phys. Lett. 100, 133505 (2012)

Electronic tuning of La2/3Sr1/3MnO3 thin films via heteroepitaxy
J. Appl. Phys. 111, 063920 (2012)

## Additional information on J. Appl. Phys.

Journal Homepage: http://jap.aip.org/
Journal Information: http://jap.aip.org/about/about_the_journal
Top downloads: http://jap.aip.org/features/most_downloaded
Information for Authors: http://jap.aip.org/authors

ADVERTISEMENT

# Strain effect caused by substrates on phase separation and transport properties in $Pr_{0.7}(Ca_{0.8}Sr_{0.2})_{0.3}MnO_3$ thin films

Y. Y. Zhao, F. X. Hu,[a] J. Wang,[a] L. Chen, W. W. Gao, J. Shen, J. R. Sun, and B. G. Shen
*State Key Laboratory of Magnetism, Institute of Physics, Chinese Academy of Sciences, Beijing 100190, People's Republic of China*

(Presented 1 November 2011; received 22 September 2011; accepted 28 November 2011; published online 9 March 2012)

Tensile and compressive strains were introduced by epitaxially growing $Pr(Ca_{0.8}Sr_{0.2})_{0.3}MnO_3$ thin films on different substrates with different lattice constants. The large tensile strain in films on $SrTiO_3$ enhances the stability of the long-range charge-orbital (CO) phase and a 5 T magnetic field cannot melt the CO phase. However, the CO phase in the film on $(LaAlO_3)_{0.3}(Sr_2AlTaO_6)_{0.7}$ (LSAT) is less robust due to a smaller tensile strain and can be partially melt by a 5T field. On the other hand, compressive strained films on $LaAlO_3$ (LAO) show different behavior. Sharp metal-insulator transition with pronounced hysteresis was observed, indicating that the long-range CO is suppressed, whereas the short-rang ferromagnetic (FM)/CO is favored. Upon magnetic field application, resistance reduces remarkably, whereas the insulator-metal (IM) transition and hysteresis becomes broader and insignificant. © *2012 American Institute of Physics*. [doi:10.1063/1.3678297]

The $Pr_{1-x}Ca_xMnO_3$ system with $0.3 \leq x < 0.75$ has a narrow one-electron bandwidth of $e_g$ band (W) and exhibits charge orbital (CO).[1] It is known that the average radius of A sites in the perovskite $ABO_3$ structure plays a key role in dominating the W and electronic characteristics. Tomioka and Tokura have shown that the random chemical replacement of Sr for Ca ($Sr^{2+}$ is larger than $Ca^{2+}$) at A sites could widen the W with the hole-doping level unchanged,[1] which was ascribed to the reduction of the $MnO_8$ octahedra distortion enhancement of the hybridization between the $e_g$ orbital and oxygen 2p orbital, due to the increase of the A site radius. As a result, the CO insulating phase partially transforms into ferromagnetic (FM) metal phase upon Sr doping. The strong competition between the CO and FM phases leads to phase separation, and an insulator-metal (IM) transition appears in a percolative manner or via linking of the separated ferromagnetic clusters,[2] depending on the introduced Sr content and the averaged radius at A sites. On the other hand, lattice effect is one of the core questions in perovskite manganites. The introduced strain by substrates directly changes the distortion of $MnO_8$ octahedra, and influences the subtle balance of free energy between the coexistent CO and FM phases and thus the transport properties. Here, we report different strain effects on the competition between CO and FM phases, phase separation, and transport properties in $Pr_{0.7}(Ca_{0.8}Sr_{0.2})_{0.3}MnO_3$ (PCSMO) thin films.

PCSMO thin films were deposited by using pulsed laser deposition technique. Targets of $Pr_{0.7}Ca_{0.3}MnO_3$ (PCMO) and PCSMO were prepared by a conventional solid phase sintering method. The commercial purities of starting powders $Pr6O_{11}$, $CaCO_3$, $SrCO_3$, and $MnO_2$ are 99.5, 99.5, 99.99, and 99.9 wt.%, respectively. To characterize the targets, a small piece of bulk was cut from their edge. X-ray diffraction (XRD) measurements, performed using Cu $K\alpha$ radiation, indicated that the bulk PCMO, PCSMO, crystallized in orthometric structure with *Pnma* space group. Magnetic and transport properties were measured by a superconducting quantum interference device VSM equipped with four-point electrical resistance technique. Figure 1 displays temperature dependent field cooling (FC) magnetization (M-T) under 0.02 T and resistivity (R-T) without magnetic field for PCMO and PCSMO bulk. Previous neutron diffraction measurements indicated that PCMO (Ref. 3) experiences charge-orbital ordering at $T_{CO} = 200$ K, antiferromagnetic ordering at $T_N = 140$ K, and canted antiferromagnetic ordering $T_{CA}$ at 110 K, whereas a similar composition $Pr_{0.7}Ca_{0.25}Sr_{0.05}MnO_3$ (Refs. 4 and 5) experiences $T_{CO}$, $T_{CA}$, and ferromagnetic ordering $T_{FM}$ in sequence with decreasing temperature. From Figs. 1(a) and 1(c), one can find that the magnetization anomaly appears at similar positions for present $Pr_{0.7}Ca_{0.3}MnO_3$ and $Pr_{0.7}(Ca_{0.8}Sr_{0.2})_{0.3}MnO_3$ bulk. It is evident that PCSMO displays a different behavior comparing with PCMO. Insulating behavior without IM transition due to long-range CO appears for PCMO [see Fig. 1(b)]. Although there is some evidence supporting the existence of FM short ordering below $T_{CA}$,[6] the FM fraction does not reach the percolation threshold and the bulk PCMO shows insulating characters. For PCSMO, its $T_{CO}$ appears at ~190 K, the bump position in M-T curve [see Fig. 1(c)]. The second bump corresponding to $T_{CA}$ appears at ~115 K. The replacement of $Ca^{2+}$ with $Sr^{2+}$ widens the $e_g$ band and long-range FM ordering develops at low temperature. The strong competition between CO and FM phases leads to a phase separation. With temperature decreases, the FM fraction reaches the percolation threshold, and IM transition with a pronounced thermal hysteresis, ~21 K, appears ~100 K [see Fig. 1(d)]. Here, we simply adopt the temperature at which R(T) peaks on cooing as $T_{FM} \sim 95$ K, in consistence with the following discussions on the $T_{FM}$ in films.

[a]Authors to whom correspondence should be addressed. Electronic mail: fxhu@iphy.ac.cn and wangjing@iphy.ac.cn.

 

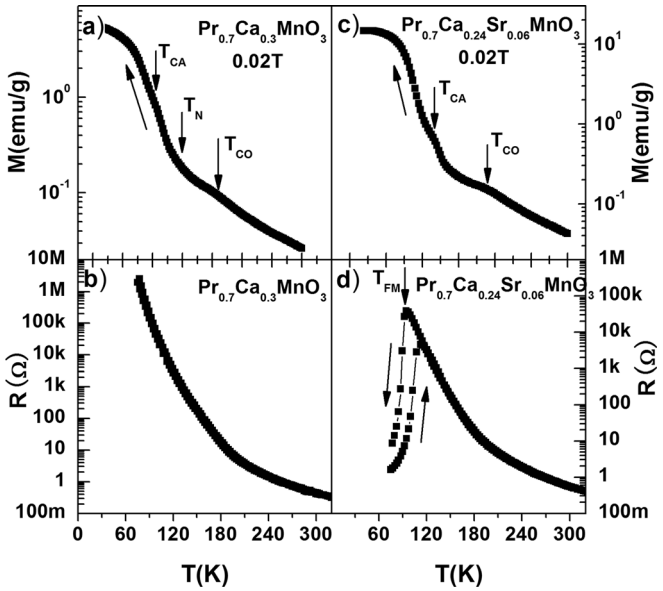


FIG. 1. Temperature dependence of FC magnetization on cooling under 0.02 T for (a) PCMO and (c) PCSMO bulk, and temperature dependence of resistivity at zero field on cooling and warming for (b) PCMO and (d) PCSMO bulk. The arrows indicate the cooling/warming path. For PCMO, $T_{CO}$, $T_N$, and $T_{CA}$ positions were defined by neutron diffraction according to Ref. 3. For PCSMO, $T_{CO}$ and $T_{CA}$ were defined as the two clear bumps at 190 and 115 K, respectively; here $T_{FM}$ simply adopts the temperature at which R(T) peaks on cooing.

Three kinds of (001) substrates with different lattice constant, $SrTiO_3$ (STO) (3.905 Å), $LaAlO_3$ (LAO) (3.788 Å), and $(LaAlO_3)_{0.3}(Sr_2AlTaO_6)_{0.7}$ (LSAT) (3.868 Å) were chosen to deposit PCSMO thin films. The target was ablated by a KrF excimer laser (248 nm) with a pulsed energy of 200 mJ and a frequency of 2 Hz. The deposition was performed at an oxygen pressure of 1 mbar and a substrate temperature of 750 °C. The film thicknesses, approximately 30, 100, and 200 nm, were controlled by depositing time. After deposition, in a pure oxygen atmosphere of 1 atm, the films were cooled to room temperature and post-annealed at 800 °C for 1 h. The crystalline structure and c-axis lattice constant were determined by x-ray diffraction measurements. It was found that the films are grown epitaxially on substrates in a single pseudocubic phase and high crystallinity. From the XRD patterns, the out-of-plane lattice parameter c was determined to be 3.928, 3.925, and 3.904 Å for 30, 100, and 200 nm films on LAO, indicating that the films undergo out-of-plane tensile strain, $\varepsilon_{zz} = (c_{film} - c_{bulk})/c_{bulk} = 2.159\%$, 2.075%, and 1.536%, respectively. By Poisson relation $\varepsilon_{xx} = -[(1-\nu)/2\nu]\varepsilon_{zz}$ ($\nu$ is the Poisson ratio), one can obtain the in-plane strain. Although $\nu$ is not known for PCSMO, typical values range between approximately 0.3 and 0.5 for most materials.[7] For a rough estimation, we chose $\nu = 0.41$, similar to the one of $La_{0.83}Sr_{0.17}MnO_3$.[8] Thus, the corresponding in-plane compressive strain could be calculated as −1.553%, −1.493%, and −1.105% for 30, 100, and 200 nm films on LAO, respectively. For the 30 and 100 nm films on STO, the out-of-plane lattice parameter c is 3.796 and 3.803 Å, indicating that the films undergo out-of-plane compressive strains of −1.281% and −1.087%, whereas in-plane tensile strains are 0.922% and 0.782%, respectively. For the 100 nm film on LSAT, the out-of-plane constant c is 3.842, smaller but close to the PCSMO bulk, indicating that the film undergoes a very small out-of-plane compressive strain of −0.084%, and an in-plane tensile strain of 0.06% (Poisson estimation). For clarity, these results are also summarized in Table I. One could expect that such different strains would cause obvious different effects on phase separation and magnetic/transport properties in the present system.

Figure 2 displays the temperature-dependent normalized resistance R(T)/R(300 K) at zero and 5 T field for (a) 100 nm PCSMO films on LSAT and STO and (b) 30, 100, and 200 nm PCSMO films on LAO compared to that of bulk. The R(T)/R(300 K) plots at zero field reveal that the tensile strained films on either STO or LSAT (100 nm) display insulating behaviors in the entire temperature range [Fig. 2(a)], indicating that the CO phase is enhanced and the percolation threshold cannot be reached in the measured temperature range. It can be noted that the resistance of both films at zero field is so large that the Keithley voltmeter can only measure the resistance down to 60 K for the film on LSAT and 120 K for the film on STO. For the film on STO, an application of 5 T field can induce a small drop of resistance (notice the small difference in the inset of Fig. 2(a) but the R-T plot still exhibits insulating behavior in the entire temperature range. This result implies that the large in-plane tensile strain (0.782% for the 100 nm film on STO) enhances the stability of the long-range CO phase, and a 5 T magnetic field could not melt the CO phase. In contrast, a 5 T magnetic field can make the CO phase in the 100 nm film on LSAT partially melt [a magnetoresistance (MR) of $3.3 \times 10^2$ was obtained at 65 K] and bulk-like percolative transport with hysteresis was observed [see Fig. 2(a)], which suggests that the CO phase in the film on LSAT is less robust due to a smaller in-plane tensile strain (0.06%). Generally, the tensile strain favors the CO phase. Our recent studies indicate that strong tensile strain can induce charge-orbital ordering even for (001)-$La_{7/8}Sr_{1/8}MnO_3$ thin film[9]. The situation of electron-

TABLE I. Summary of substrate and PCSMO film properties, c-axis lattice constant, and out-of-plane and in-plane strains.

| Substrate | Lattice constant of substrate(Å) | Lattice constant of bulk (Å) | Film thickness (nm) | c-Axis lattice constant (Å) | Out-of-plane strain (%) | In-plane strain (%)[a] |
|---|---|---|---|---|---|---|
| $LaAlO_3$ | 3.788 | 3.845 | 30 | 3.928 | 2.159 | −1.553 |
| | | 3.845 | 100 | 3.925 | 2.075 | −1.493 |
| | | 3.845 | 200 | 3.904 | 1.536 | −1.105 |
| LSAT | 3.868 | 3.845 | 100 | 3.842 | −0.084 | 0.060 |
| $SrTiO_3$ | 3.905 | 3.845 | 30 | 3.803 | −1.281 | 0.922 |
| | | 3.845 | 100 | 3.796 | −1.087 | 0.782 |

[a]Poisson estimation.

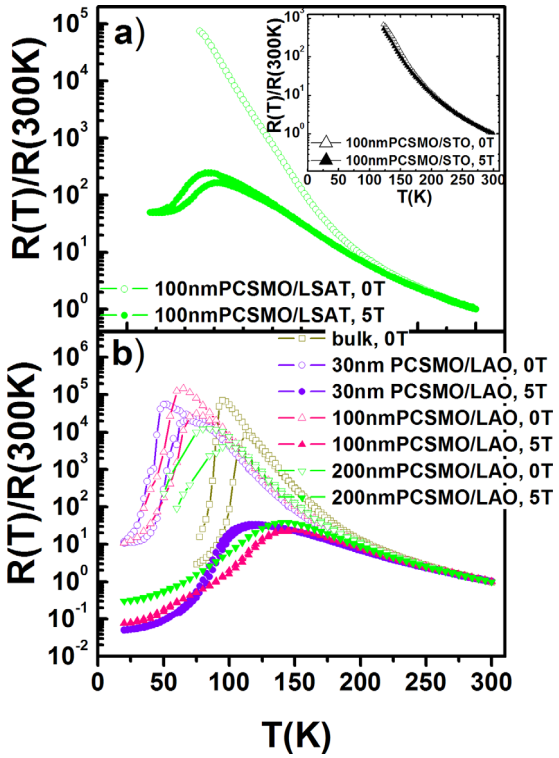


FIG. 2. (Color online) The dependence of normalized resistivity on temperature under 0 and 5 T for (a) 100 nm PCSMO films on LSAT and STO, (b) 30, 100, and 200 nm PCSMO films on LAO compared to that of bulk.

lattice coupling plays a crucial role for the subtle balance of phase separation and the stability of CO phase in the present samples. One particular mechanism for the electron-lattice coupling is the Jahn-Teller (JT) distortion of the $MnO_6$ octahedrons, which lifts the degeneracy of the Mn $e_g$ levels by biaxial distortion and results in the self-trapping of the charge carriers into a polaronic state. The introduced strain by substrates could change the JT distortion and thus the strength of the CO phase. A tensile strain would compress the $MnO_6$ octahedrons in an out-of-plane direction with simultaneous elongation in the in-plane direction. The enhanced JT distortion may assist CO and tends to restrict the carriers in a local distorted lattice,[10] leading to the appearance of insulating behavior.

On the other hand, compressive strained films on LAO show different behavior. Figure 2(b) shows the dependence of normalized resistivity on temperatures under 0 and 5 T for the films (30, 100, and 200 nm) on LAO compared with that of bulk. Sharp metal-insulator transition with pronounced hysteresis was observed for all the films on LAO, implying that the long-range CO is suppressed and the short-rang FM/CO is favored at low temperature. Upon magnetic field application, resistance reduces remarkably, whereas the IM transition and hysteresis becomes broader and insignificant, indicating that the CO phase is melted into the FM phase and the phase separation becomes trivial under magnetic fields. One can notice that the resistivity under 5 T becomes temperature reversible without hysteresis across the IM transition for 100 and 200 nm films on LAO, which suggests that the CO fraction has transformed into the FM phase and FM ordering dominates the transport at low temperature. A large

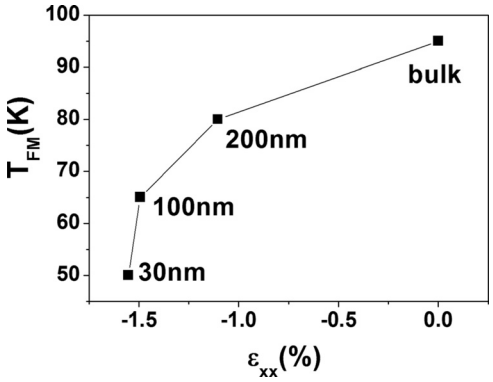


FIG. 3. Dependence of transition temperature $T_{FM}$ on in-plane strain for the films on LAO (the line guides the eyes). Here $T_{FM}$ simply adopts the temperature at which R(T) peaks on cooing in Fig. 2(b).

magnetoresistance (MR) effect was observed due to such a transition driven by the magnetic field. The MR under 5 T reaches 6.1, 4.3, and $3.1 \times 10^5$ at 80, 65, and 50 K for 200, 100, and 30 nm films on LAO, respectively. Magnetic measurements revealed that both the $T_{FM}$ and $T_{CA}$ transitions, similar to that of bulk, remain for the films on LAO. As for the CO point, it is invisible in the M-T curves, which is usual for such films. However, transport and neutron diffraction measurements[11] support the existence of CO ordering. Figure 3 displays the dependence of transition temperature $T_{FM}$ on the in-plane strain for the films on LAO (the line guides the eyes). For simplicity, here we adopt the temperature at which R(T) peaks on cooing as $T_{FM}$ [see Figs. 1(b) and 2(b)]. The $T_{FM}$ behaves highly sensitive to in-plane strain as the thickness is smaller than 200 nm. With increasing the thickness, the strain gradually relaxes and the $T_{FM}$ increases rapidly and approaches to that of bulk. Usually, the in-plane isotropic strain induces tetragonal lattice distortion and diminishes original orthometric structure in the bulk. However, the in-plane compressive strain will cause a reduction of the in-plane Mn-O-Mn bond distance and relieve the $MnO_6$ octahedral distortion. As a result, the in-plane transfer integral from double exchange coupling enhances, and FM ordering increases. The CO phase loses its stability and transforms into the FM phase under a magnetic field, exhibiting a large MR effect.

This work has been supported by the National Natural Science Foundation of China, the National Basic Research of China, and Beijing Natural Science Foundation of China.

[1]Y. Tomioka *et al.*, Phys. Rev. B **66**, 104416 (2002).
[2]M. Uehara *et al.*, Nature **399**, 560 (1999).
[3]H. Yoshizawa *et al.*, Phys. Rev. B **52**, R13145 (1995).
[4]A. Maignan *et al.*, J. Magn. Magn. Mater. **153**, 260 (1996).
[5]J. Hejtmanek *et al.*, Phys. Rev. B **54**, 11947 (1996).
[6]A. Maignan *et al.*, J. Magn. Magn. Mater.**168**, L237 (1997).
[7]S. P. Timoshenko *et al.*, *Theory of Elasticity* (McGraw-Hill, New York, 1987), Chap. 2.
[8]T. W. Darling *et al.*, Phys. Rev. B **57**, 5093 (1998).
[9]J. Wang *et al.*, Appl. Phys. Lett. **96**, 052501 (2010).
[10]A. J. Mills *et al.*, Phys. Rev. Lett. **74**, 5144 (1995).
[11]R. C. Budhani *et al.* Phys. Rev. B **65**, 014429 (2001).